Ref. Ares(2025)34755 - 05/01/2025

HEFT

D4.2 Electromagnetic and Performance. Design Report of Motor for Class C+D+E Vehicles

Funded by
the European Union

Call	HORIZON- CL5-2020-D5-01	
GA Number	101096306	
Deliverable No.	D4.2	
Deliverable Title	Electromagnetic and performance. Design report of motor for class C+D+E	
Deliverable Date	2025-01-05	
Contractual delivery	2024-05-31	
Deliverable Type	R	
Dissemination level	PU	
Status	V2.0	2025-01-05

Written By	Gaizka Almandoz	2024-11-27
Checked by	Iago Martinez	2024-12-16
Approved by	Javier Poza	2025-01-05

HORIZON CL5-2020-D5-01. HEFT 101096306 – Novel concept of a Low Cost, High Power Density and Highly Efficient Recyclable motor for next generation mass produced electric vehicles

Acknowledgement:

The author(s) would like to thank the partners in the project for their valuable comments on previous drafts and for performing the review.

Project partners:

1. MGEP (Mondragon Goi Eskola Politeknikoa Jose Maria Arizmendiarrieta S Coop).
2. GKN (GKN Driveline Zumaia SA).
3. GKN AIC (GKN Automotive Innovation Center - GKN Hybrid Power Ltd.).
4. MAGNETI (Magneti Ljubljana d.d.).
5. VYNCOLIT (Vyncolit N.V.).
6. IKERLAN (IKERLAN S. Coop.).
7. UNIBO (Alma Mater Studiorum - Università di Bologna).
8. KUL (Katholieke Universiteit Leuven).
9. UoN (University of Nottingham).

Disclaimer:

This project has received funding from the European Union's Horizon Europe research and innovation programme under grant agreement No 101096306. Funded by the European Union. Views and opinions expressed are however those of the author(s) only and do not necessarily reflect those of the European Union, the European Commission or the European Climate, Infrastructure and Environment Executive Agency (CINEA). Neither the European Union nor the granting authority can be held responsible for them.

1 EXECUTIVE SUMMARY 5
2 DESIGN PROCESS 6
2.1 DESIGN METHODOLOGY 6
2.1.1 Preliminary Sizing *6*
2.1.2 Optimization *6*
2.2 EVALUATION OF MOTOR PERFORMANCES 7
2.2.1 Peak Torque/Power envelopes *7*
2.2.2 Continuous Service *7*
2.2.3 Demagnetization Risk in Magnets *7*
2.2.4 Evaluation of KPIs (Key Performance Indicators) *8*
3 PRELIMINARY SIZING OF THE MOTOR 9
3.1 DESIGN CONSTRAINTS 9
3.2 DESIGN OF THE STATOR 10
3.3 DESIGN OF THE ROTOR 12
4 OPTIMIZATION OF THE ROTOR 14
4.1 ELECTROMAGNETIC OPTIMIZATION 14
4.1.1 Definition of the optimization process *14*
4.1.2 Pareto's of the optimization process *15*
4.2 EVALUATION OF THE MECHANICAL PERFORMANCES 16
4.3 REDUCTION OF THE ROTOR WEIGHT 17
5 CONTINUOUS SERVICE PERFORMANCE 18
5.1 COMPUTATION OF LOSSES 18
5.1.1 Copper losses *18*
5.1.2 Iron losses *19*
5.1.3 Magnet losses *19*
5.2 COOLING SYSTEM 19
5.3 CONTINUOUS SERVICE CURVES 20
6 FINAL PERFORMANCES AND COMPUTATION OF KPIS 22
6.1 EVALUATION OF KPIS 22
6.1.1 Computation of Weight and Volume *22*
6.1.2 Evaluation of Torque and Power Densities *24*
6.1.3 Evaluation of the REE Saving *25*
6.2 25
6.3 FINAL PERFORMANCES 26
7 DELIVERY DEVIATIONS FROM THE INITIAL PLANNING 29
8 CONCLUSIONS 30

GLOSSARY

Abbreviation/ acronym	Description
MTPA	Maximum Torque per Ampere
MTPV	Maximum Torque per Voltage
GA	Grant Agreement
KPI	Key Perfomance Indicator

1 EXECUTIVE SUMMARY

Climate change has created an increased need for innovation in various sectors, including the automotive industry. Many corporations are striving to fulfil this need by developing and producing electric cars. However, the production process remains inefficient and environmentally harmful. The EU-funded HEFT project will reverse this trend by introducing a revolutionary synchronous motor for electric cars, which will be recyclable, cost-efficient and require fewer materials while producing fewer emissions and creating novel European circular economies.

HEFT Project proposes a set of innovation challenges on electric synchronous motor configuration based on SiC inverters (direct cooling of rotor and stator, advance insulation for high voltage, multibarrier rotor topology, wave windings) and advanced materials (advanced GBD magnets, epoxy for magnet fixation, composite for motor housing, insulation resin). These innovations will result in a high-efficient and low-cost solution that will be validated on 2 motor topologies.

- Motor topology type C: Motors for C-D-E vehicle segments.
- Motor topology type A: Motors for A-B vehicle segments.

In this document the work carried out in Task 4.2 of HEFT project has been summarized. An ultra-light motor design for segment C+D+E is developed. The multi-layer rotor topology makes possible to reduce de usage of permanent magnet leading to an important saving in the rare earth elements. Wave winding techcnology allows to develop compact and efficient stator. End winding length is reduced and high frequency losses are reduced in the copper. Involving all these techonologies a high power density motor is developed.

In this document the following issues will be covered:

1. Design Process (Design Methodology and Procedure to motor performances evaluation).
2. Preliminary sizing of the motor.
3. Optimization of the rotor
4. Continuous service evaluation.
5. Final performances evaluation and KPIs computation.

2 DESIGN PROCESS

2.1 Design Methodology

The applied design methodology is the same as the one applied in the case of segment AB. It consists of 3 main stages as it is shown in Figure 1. In the first stage the stator geometry, the magnet grade, and the different rotor topologies to be considered are defined. In the second stage all these rotor topologies are sized in order to fulfil the specifications. As a result of this stage, preliminary design proposals are obtained, and finally these proposals are optimized in the third stage, applying genetic optimization algorithms.

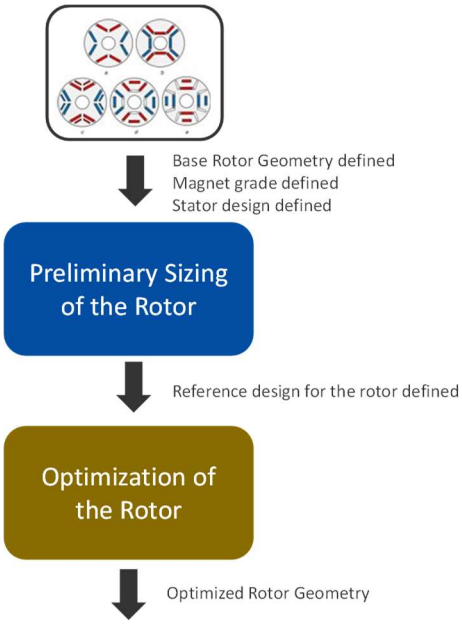

Figure 1. Flow chart of the applied design process

2.1.1 Preliminary Sizing

A first approach is carried out for each rotor topology, adjusting manually the 2D geometries and the stack length, trying to improve as much as possible the performances and the KPIs.

In this particular case only one rotor topology is considered. As a result of the design process of AB eMotor, the so-called V Block topology has been identified as the best one. Hence, in the case of CDE segment only this topology is considered.

2.1.2 Optimization

A genetic algorithm is employed to conduct the optimization process, with the rotor geometry being parameterized. A sensitivity analysis is performed to identify the most significant design parameters, which are subsequently adjusted using the genetic optimization algorithm.

The following objectives have been established for the optimization:

- To maximize the power density as much as possible
- To minimize the magnet weight
- To reduce the torque ripple as much as possible

In addition, the following constraints have been considered:

- Demagnetization Ratio: 4% (it is calculated suppling 350A in the d-axis, being q-axis current zero, and at 120ºC)
- Meet the peak torque envelop with the maximum current

2.2 Evaluation of Motor Performances

2.2.1 Peak Torque/Power envelopes

The peak torque envelop is obtained considering the maximum current of 350A and applying the Maximum Torque per Ampere (MTPA) strategy up to the base speed. At the base speed the supplying voltage reaches the maximum allowed value (defined by the inverter, in this case 265V rms per phase), and from this speed the applied strategy is the maximum torque per voltage (MTPV). The maximum power envelop is obtained multiplying the maximum torque and the speed.

2.2.2 Continuous Service

The continuous service is defined as the steady state working point. At each specified operation speed the steady state operation mode is computed limiting the working temperatures to 180ºC for the winding and 140ºC for the magnets. As in the same way done for the maximum envelope, for the computation of continuous service working points the MTPA strategy is applied while the supplying voltage is below the maximum allowed value. In case the maximum voltage value is reached MTPV strategy is applied.

2.2.3 Demagnetization Risk in Magnets

Besides fulfilling the specified working points, the motor must withstand all working points without losing the energy stored in the magnets. The maximum torque/power envelopes are considered to be the worst operating points concerning the risk of demagnetization in the magnets. In order to assure the integrity of the magnets in the entire operating map the working point of the magnets is analysed over the peak envelop.

The characteristic curve of the magnet is considered at the working temperature. In this case 150ºC is defined as the working temperature to evaluate the demagnetization. The demagnetization knee point over the characteristic curve of the magnet must be considered. In case of magnets grade N42SH, the knee point is situated at $B = 0.37\ T$ (see Figure 2).

It must be assured that the working point of all magnets is above this knee point over all peak torque envelop to avoid the risk of demagnetization.

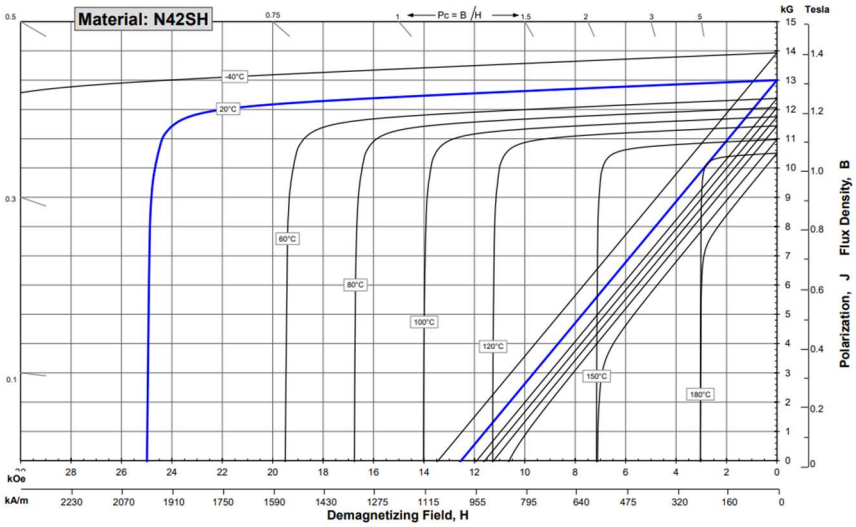

Figure 2. Characteristic curves of magnets N42SH at different working temperatures

2.2.4 Evaluation of KPIs (Key Performance Indicators)

During the different design iterations, the following KPIs were evaluated: (1) power and torque density during continuous service (Kw/Kg, Kw/l, Nm/Kg, Nm/l) and (2) savings in rare earth materials relative to the motor benchmark. The methodology for obtaining these KPIs is detailed in Section 6.

3 PRELIMINARY SIZING OF THE MOTOR

Following the design procedure defined in Figure 1, first the 2D drawing of the stator has been defined. Then the rotor design has been accomplished.

3.1 Design Constraints

The number of pole pairs is set to $p = 3$ to limit the supplying frequencies. It is well established that, for a given mechanical speed, an increase in the number of poles results in a higher supply frequency.

The V Block rotor geometry has been selected, as it has been identified during the AB eMotor design process as the optimal configuration. Consequently, no alternative designs are considered in this instance.

Skewing will be implemented to reduce torque ripple. Additionally, further techniques used in the AB motor can also be applied to further minimize torque ripple. For example, magnetic wedges will be incorporated into the opening regions of the stator slots.

Wave winding technology is essential for this design. The advantages of this technology over conventional hairpin winding will aid in achieving the KPIs.

The stator design of the AB motor serves as a reference to simplify the manufacturing process, with three degrees of freedom established: the stator outer diameter, the number of layers or conductors within the slots, and the stack length.

The stack length is defined as a degree of freedom. However, preliminary analysis suggests that the stack length should be in the range of 85 mm to 120 mm to meet the power density KPI.

An oil cooling system will be implemented. Heat will be extracted from the rotor via a spiral groove in the shaft and through core cooling channels, while the end windings will utilize spray cooling technology. This cooling system is expected to support a maximum current density of 42 A/mm².

The design will utilize N42SH grade magnets. The benchmark motor employs magnets with a higher thermal grade. By opting for a lower thermal grade, the requirement for heavy rare earth elements (HREE) is reduced, thereby contributing to the REE savings KPI.

The thermal class of the stator windings is Class H (180°C), which aligns with the typical thermal class used in electric vehicles.

Geometry	Pole Pairs	3
	Stator ID	134 mm
	Airgap	0.8 mm
Active Parts	Rotor Skew Angle	1.67° (4 sectors)
	Electrical Steel Grade	NO 27
	Magnet Grade	N42SH
	Cooling Circuit Design	Oil Cooling through rotor Spray oil cooling
Winding	Winding connections	3Y – Full Pitch
	eMotor thermal class	Class H (180°C)
	Peak Current Density	42 A/mm^2

Table 1. Main Design Constraints

3.2 Design of the Stator

The stator of the AB eMotor is used as a reference, allowing for modifications to only three variables:

- The stator outer diameter
- The number of layers or conductors inside the slot
- The stack length.

The AB stator consists of 54 slots. As shown in Table 2, there are initially three alternatives for the number of layers and parallel circuits corresponding to these 54 slots. For the CDE motor, the base speed requirement is higher than that of the AB motor. If we adopt the same configuration as the AB motor—12 layers with 3 parallel circuits (36 turns per phase)—it may be challenging to meet the base speed torque requirement of the CDE motor. Reducing the number of turns per phase would facilitate compliance with the base speed torque requirement.

Furthermore, decreasing the number of layers will reduce the amount of copper used, which in turn will decrease the stator outer diameter, resulting in a lighter stator. This reduction is crucial for achieving the power and torque density KPIs. Therefore, the configuration of 10 layers with 3 parallel circuits has been selected for the CDE eMotor. Notably, this configuration is the most robust option according to Table 2.

Continuos winding possible configurations				
Q	Layers	Parallels	Nph	Symmetry
36	6	1	36	Strong
		2	18	Strong
	8	1	48	Strong
		2	24	Strong
	10	1	60	Strong
		2	30	Strong
	12	1	72	Strong
		2	36	Strong
72	6	1	72	Strong
		2	36	Strong
	8	1	120	Strong
		2	48	Strong
		4	24	Weak
	10	1	120	Strong
		2	60	Strong
54	10	3	30	Strong
	12	3	36	Strong/Weak
		1	108	Weak

Table 2. Feasible stator solutions for p=3

Another configuration, initially not included in Table 2, has also been evaluated. By slightly modifying the manufacturing process—specifically, by splitting the mat into two parts and connecting both parts in parallel—it is possible to define an alternative configuration comprising 8 layers and 2 parallel circuits. Although the resulting turns per phase are the same as in the AB eMotor, the reduced number of conductors leads to a lighter stator.

However, simulation results indicate that this configuration is not feasible due to the generation of relatively high circulating currents among the parallel paths, which can result in increased noise, vibrations, and losses. Figure 3 illustrates the imbalance between the currents in the two parallel paths. One path carries approximately 120 A, while the other carries less than 50 A. This significant imbalance arises because transposition of the conductors is not possible; consequently, all conductors in one path are positioned at the top of the slot, while those in the other path are located at the bottom. As a result, the impedances of the two parallel paths differ significantly, leading to this substantial current imbalance.

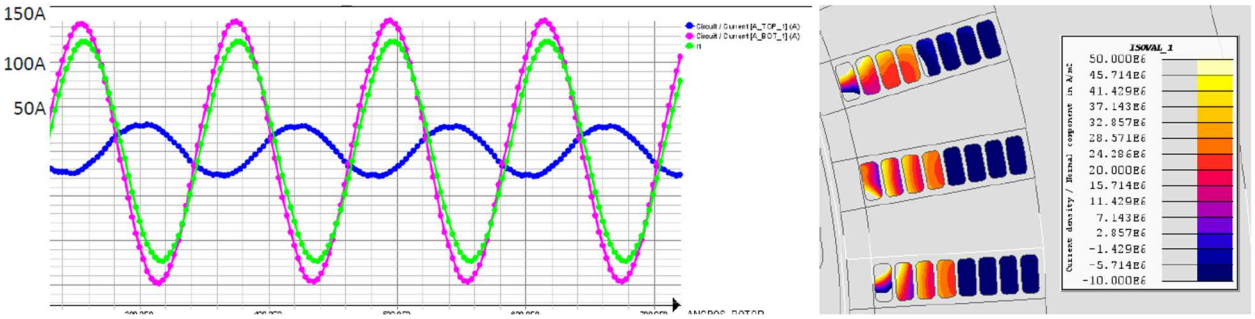

Figure 3. Total phase current (pink) and the currents distribution among the two parallel paths (green and blue). Current density distribution in the two parallel paths conductors (right side picture)

As the next step, the dimensions of the stator geometry are defined by considering the following aspects:

- **Degrees of freedom**: The only degrees of freedom are the height of the teeth and the stator yoke
- **Yoke height**: a good trade-off between magnetic saturation of the yoke and the motor weight must be found. The yoke height must be sufficient to prevent magnetic saturation; however, increasing the height will also increase the weight of the stator.
- **Teeth height**: The height of the teeth is equivalent to the slot height. Once the conductor size (identical to that used in the AB eMotor) and the number of layers are established, the slot and teeth height can be determined.

Figure 4 illustrates the defined 2D drawing of the stator.

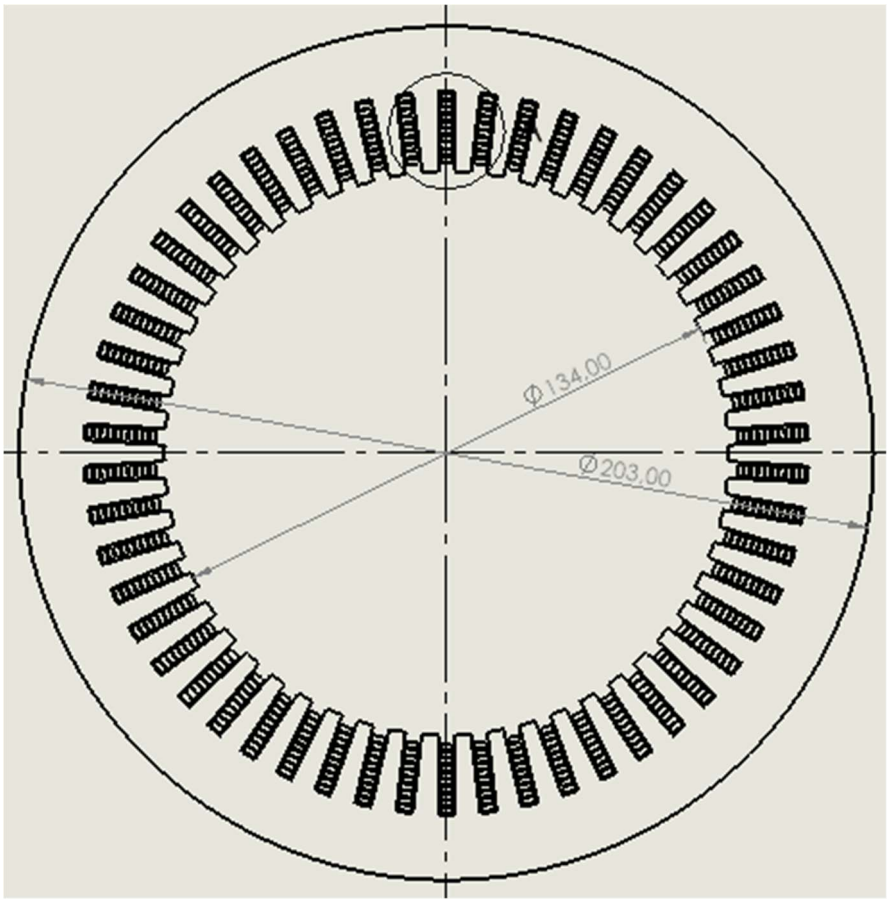

Figure 4. 2D drawing of the designed stator. 10 layers / 3 parallel paths

3.3 Design of the Rotor

The V Block rotor topology has been selected for consideration. During the design process of the AB segment eMotor, it was determined that the V Block topology is the optimal solution among all evaluated alternatives.

Using the rotor of the AB segment eMotor as a reference, the new rotor is sized to meet the peak torque requirements of the CDE segment. The dimensions of the magnets are adjusted to achieve the necessary specifications.

The peak and continuous operating points are evaluated. The peak torque curve is primarily influenced by the magnetic design, while the continuous operating point is largely determined by thermal performance, with the cooling system and losses being the key factors.

To minimize the mass of the active components, the stack length is set to 100 mm. Reducing this length further would not satisfy the peak torque requirement. Once the stack length is established, the rotor dimensions are initially calculated based on the following criteria:

- **Magnet Volume**. For a given current value and a given stator configuration, the peak torque capability is dependent on the magnetic flux generated by the magnets. It is essential to enhance the effectiveness of the magnets to achieve maximum magnetic flux with minimal magnet volume.
- **Working Temperatures**. Maximum temperatures are constrained to 180°C for copper and 120°C for magnets for the computation of the peak service.
- **Demagnetization**. The risk of demagnetization can be mitigated by adjusting the height of the magnets. Higher magnets provide greater resistance to demagnetization. A balance must be struck between minimizing demagnetization risk and optimizing magnet volume.

Figure 5 illustrates the resulting torque and power peak envelope for the V-Block rotor layout. It is evident that the peak torque specification is fulfilled across the entire operating range, with a particularly significant margin at high speeds. This is due to the base speed being considerably higher than the value required for the application. Consequently, the peak power capability of the motor exceeds the application's requirements.

Figure 6 illustrates the operation of the magnets at the working point WP1, with results obtained at a magnet temperature of 120°C. As shown, the operating point of the magnets is positioned above the knee point (located at 0.369 T) across all magnet regions. Therefore, it can be concluded that there is no risk of demagnetization for the magnets.

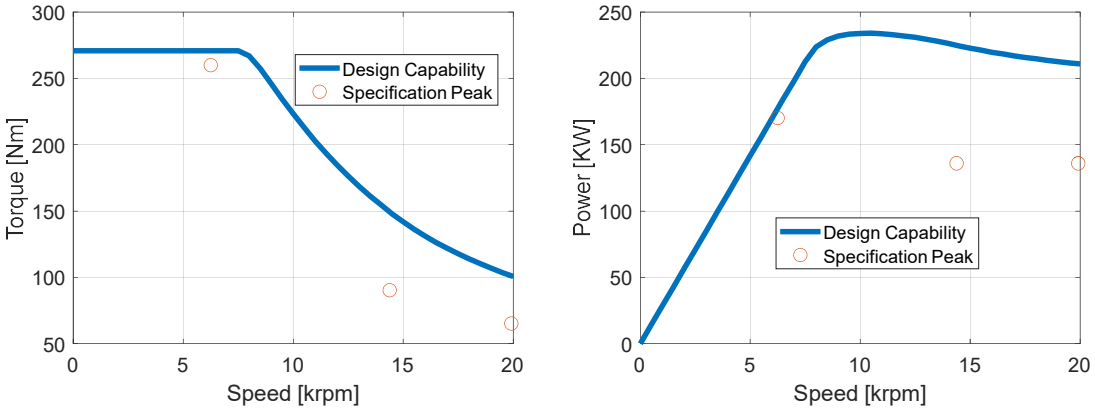

Figure 5. Torque and Power peak envelopes for the V-Block rotor layout at 180ºC in the winding and 120ºC in the magnets

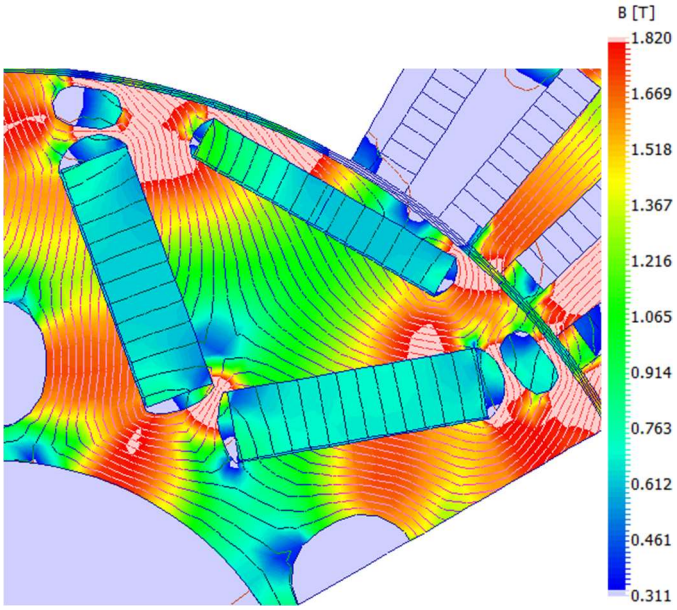

Figure 6. Operating point of the magnets at the working point WP1 (6250 rpm / 260 Nm) / 120ºC in the V-Block rotor layout

The pole pitch has been adjusted to minimize torque ripple as much as possible. Additionally, the rotor has been skewed (with four slices), and magnetic wedges have been added in the slot opening region. With these design considerations, the maximum torque ripple is maintained at approximately 10%. However, as shown in the Figure 7 there are specific working points (WP2 and WP3) where the torque ripple exceeds 10%. Following the optimization process, the torque ripple is reduced to below 10% (see next chapter)

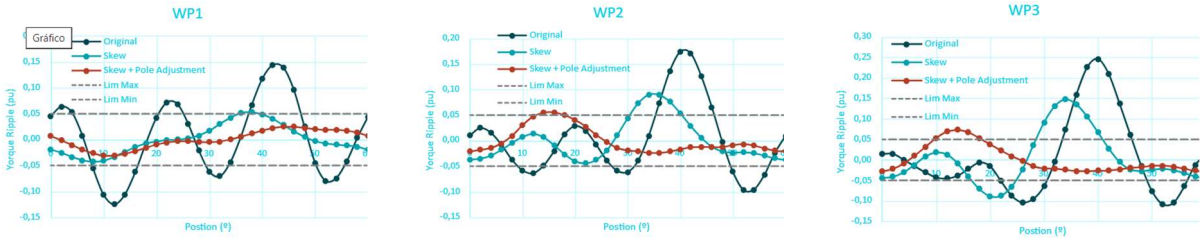

Figure 7. Torque ripple computed at different working points, before and after adjusting the pole pitch, with and without skewing of the rotor. Magnetic wedges are included in all cases

4 OPTIMIZATION OF THE ROTOR

After defining the preliminary rotor designs, the next stage focuses on design optimization (refer to the design methodology illustrated in Figure 1).

4.1 Electromagnetic Optimization

4.1.1 Definition of the optimization process

Electromagnetic multi-objective optimization of the rotor is conducted to enhance the performance and key performance indicators (KPIs) of the motor. Table 4 summarizes the objectives and constraints of the parametric optimization.

Objectives	Constraints
Maximize the mechanical peak power Minimize the magnet weight Minimize the torque ripple	Meet torque-speed requirement with $350\ A_{rms}$ Demagnetization ratio at $id = 350A\ /\ T_{magnet} = 120ºC$, <4%

Table 3. Definition of the optimization strategy. Objectives and constraints.

To reduce computational load and accelerate the optimization process, the mechanical power calculated at base speed is considered for maximization. While this does not represent the maximum power along the peak envelope, it serves as a valid reference for the optimization process. Accurately computing the maximum power value in each iteration would significantly increase the computational load.

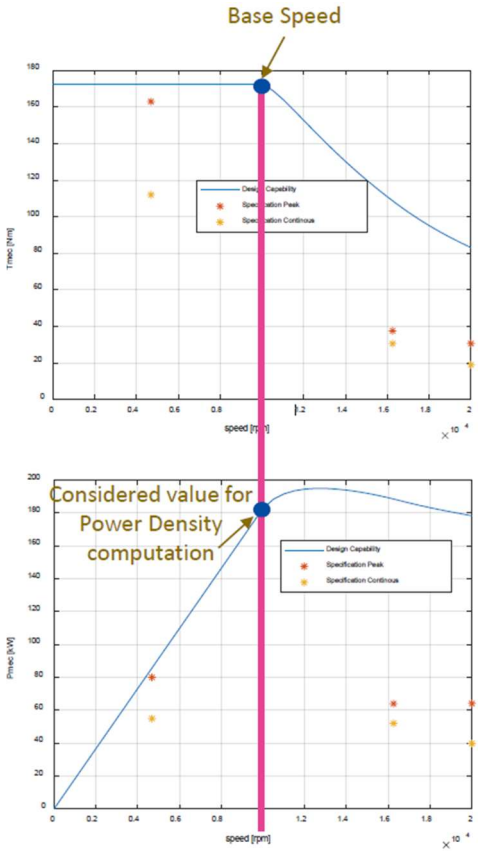

Figure 8. Mechanical power at base speed considered as the maximum power in the optimization process

4.1.2 Pareto's of the optimization process

In the Figure 9 and the Figure 10 the Pareto frontiers obtained from the multi-objective optimization are shown. To select the best candidates from these Pareto fronts, the following criteria are applied:

- **Criterion 1:** Discard all candidates with a magnet weight greater than 1.8 Kg. This ensures a minimum magnet weight saving of 34% (see Figure 11)
- **Criterion 2:** Discard all candidates with a torque ripple greater than 5%. The worst-case scenario occurs at working point 3 (19,914 rpm / 65.2 Nm). Although the torque ripple requirement allows for a maximum of 10%, the threshold is set to 5% in this case due to the assumption of computational error during the optimization process. To reduce computational load, the number of simulated points per torque ripple period is decreased, which may lead to a higher error in the torque ripple estimation (see Figure 11)
- **Criterion 3:** Chose the candidate with the higher mechanical power. Once criterion 1 & 2 are applied, among the remaining candidate the one with the higher mechanical power is chosen in order to maximize the power density.

It must be underlined that the computed maximum power densities in all cases are slightly smaller than the real ones due to the fact that during the optimization process the power densities are calculated considering the power values at base speed (slightly smaller than actual maximum values). Hence, when the performances of the final rotor are evaluated more in detail in the next section, the resulting power density is sort of higher.

The final selected candidate is highlighted in Figure 12 with a green marker. It is evident that, in terms of torque ripple and maximum mechanical power, there are candidates that may perform better than the chosen one (as indicated by the candidates marked in red). However, all these alternatives were ultimately discarded because they do not meet the demagnetization constraint.

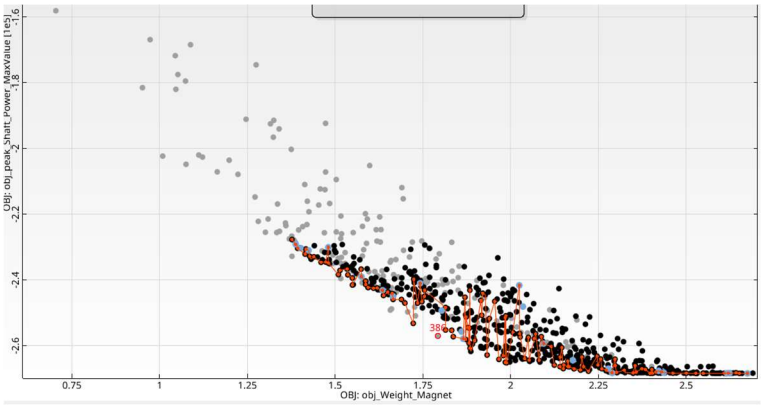

Figure 9. Obtained Pareto Frontier from the multi-objective parametric optimization process. Max Mechanical Power vs Magnet Weight

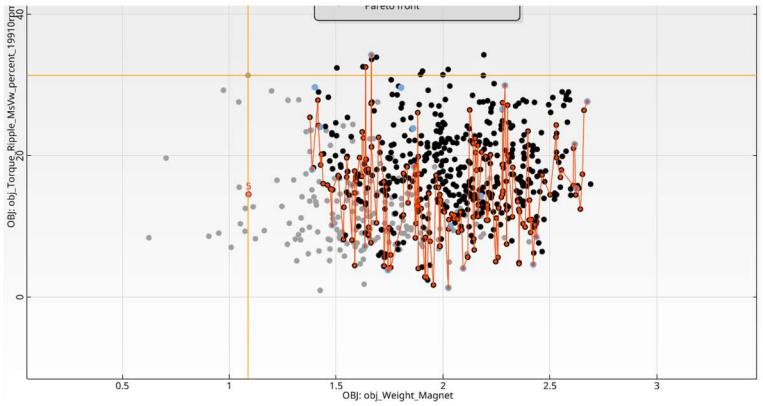

Figure 10. Obtained Pareto Frontier from the multi-objective parametric optimization process. Torque Ripple vs Magnet Weight

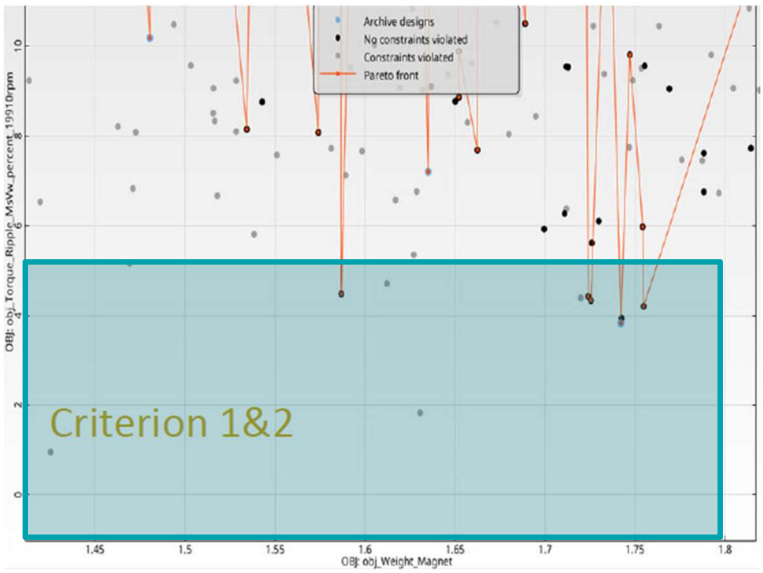

Figure 11. Selection of all candidates from the Pareto Frontier applying the criteria 1&2. Pareto Frontier relating torque ripple with magnet weight

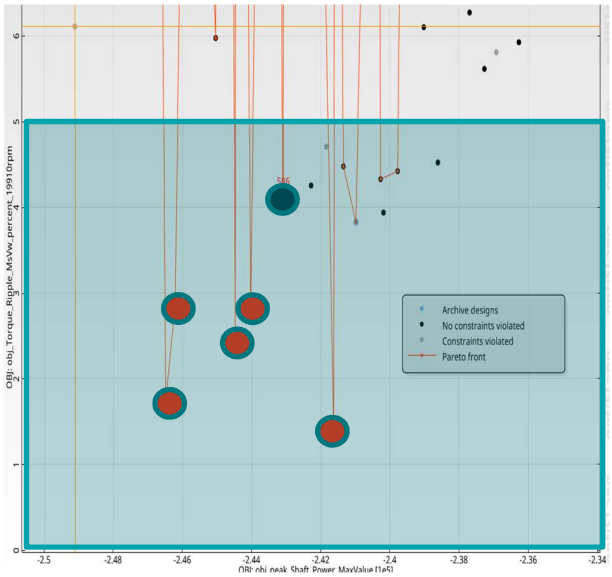

Figure 12. Selection of all candidates from the Pareto Frontier applying the criteria 1&2. Pareto Frontier relating torque ripple with Max Mechanical Power. The chosen candidate (Green) and the discarded candidates due to demagnetization risk (Red)

4.2 Evaluation of the mechanical performances

Once the rotor is electromagnetically optimized, then the mechanical stresses are evaluated. The motor must be function at relatively high speeds, up to 20.000 rpm, so the robustness of the rotor structure must be analysed. For that purpose, the mechanical stress simulations are conducted at the maximum speed of 20.000 rpm, and it is concluded that in some region the mechanical stress is over the maximum limit (400 MPa for electric steel of grade NO 27). In order to reinforce the rotor structure and reduce the mechanical stress, the following design modifications are implemented:

- **Modification 1:** The width of the outer layer bridge is increased by 0.5 mm
- **Modification 2:** The width of the inner layer bridge is increased by 0.5 mm
- **Modification 3:** The width of the outer layer magnet is decreased by 0.5mm

In the Figure 13 the peak curves are compared before and after accomplishing the rotor geometry modifications. As it can be seen, the peak curve performance hardly changes.

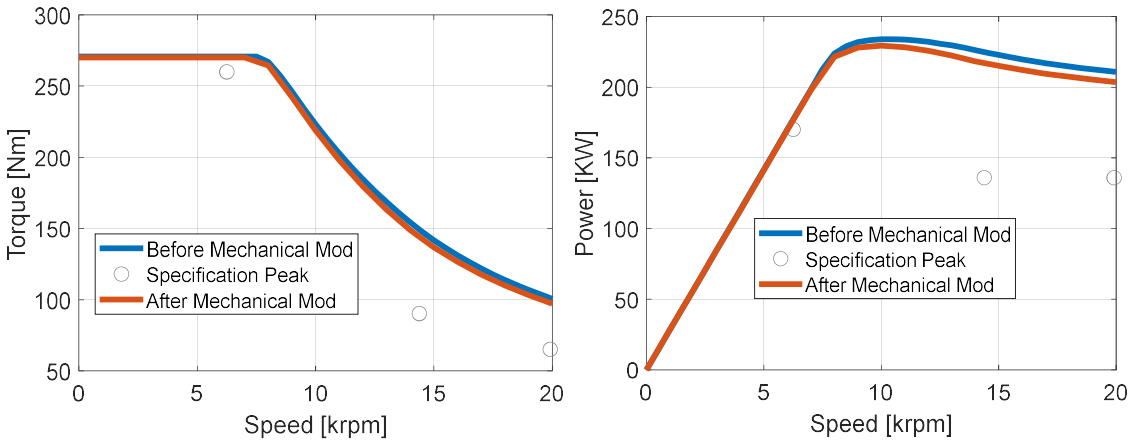

Figure 13. Torque and Power peak envelopes for the V-Block rotor layout at 180ºC in the winding and 120ºC in the magnets. Before and after geometrical modifications of the rotor to reduce the mechanical stresses

4.3 Reduction of the rotor weight

The rotor yoke is not magnetically saturated. Due to that, material can be removed from this region in order to make the rotor lighter. Adding these holes, the weight of the rotor laminations is reduced from 5.87 Kg to 5.38 Kg.

This rotor modification has minimal impact on the peak curve performance, as illustrated in the Figure 14. While it is true that performance decreases slightly, the specifications are still met with a considerable margin.

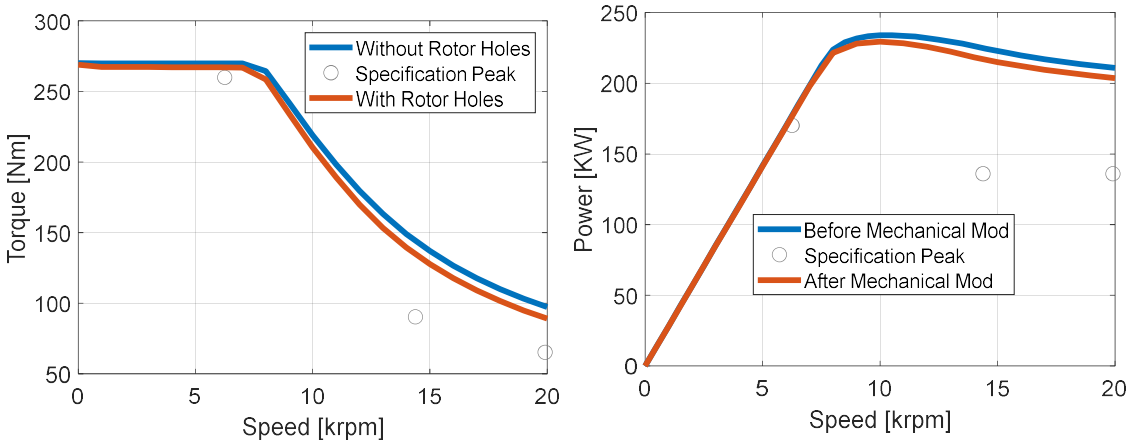

Figure 14. Torque and Power peak envelopes for the V-Block rotor layout at 180ºC in the winding and 120ºC in the magnets. Before and after geometrical modifications of the rotor to reduce the mechanical stresses.

5 CONTINUOUS SERVICE PERFORMANCE

In this section the continuous service of the designed motor is evaluated. First the overall losses of the electrical motor are evaluated, and after these losses are introduced to the thermal simulations in order to evaluate the thermal performance of the motor. This way the continuous service curve is obtained.

5.1 Computation of losses

The losses are computed considering PWM voltages. A time step simulation of the motor is carried out in MATLAB-SIMULINK and the steady-state current waveforms are obtained at each working point. Then this current waveform is used to drive the FEA simulation and the overall losses of the motor are computed. The motor model used in time step simulations is based on flux maps defined by FEA simulations of the motor. This procedure is depicted in the Figure 15.

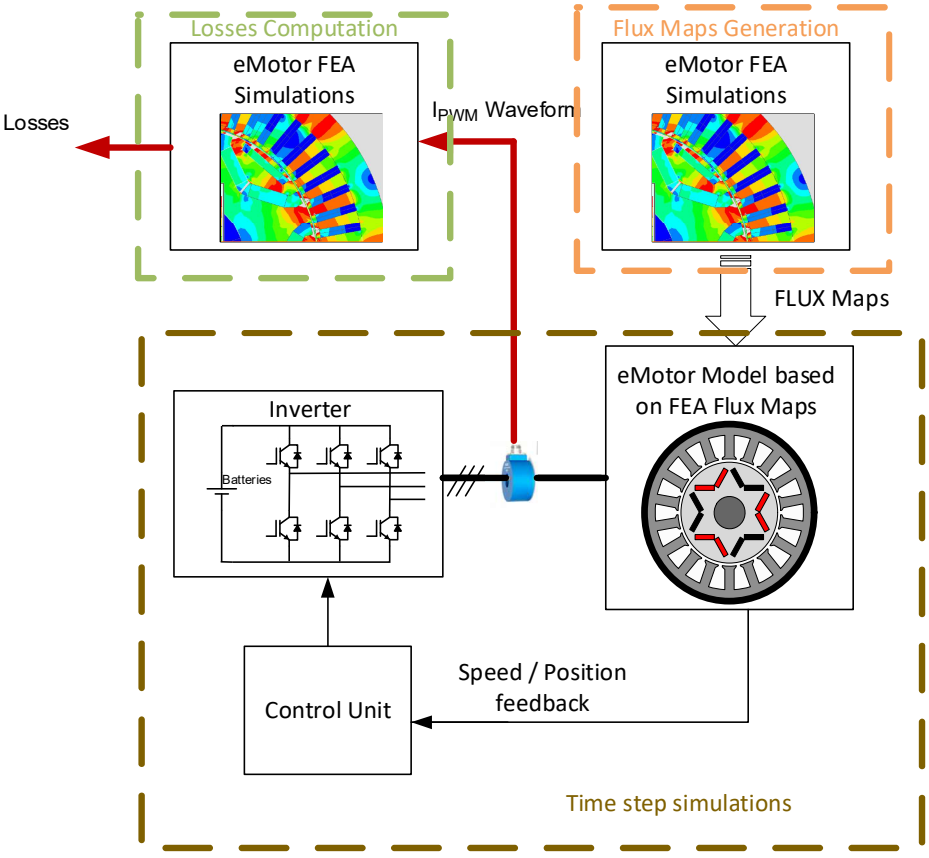

Figure 15. Procedure for losses computation accounting for PWM voltages

5.1.1 Copper losses

In low frequency operation the so-called AC copper losses are negligible but at high frequencies these losses might be taken into consideration. In this case the operating frequencies might reach up to 1000 Hz. At this level the skin and proximity effects arise, and AC losses might become relevant. As it is described in the deliverable D4.1, at the maximum operating speed the total copper losses might increase 150% due to the effect of AC losses. This resistance increase is because a non-uniform distribution of the current in the conductors, which become more relevant at high frequencies and is due to skin and proximity effects.

5.1.2 Iron losses

The iron losses are computed using the widely known Bertotti's model. The total iron losses are exploited in three components: hysteresis losses, Eddy losses and Excess losses. Each component is modelled by an analytical expression as it was described in the deliverable D4.1.

5.1.3 Magnet losses

Losses in the magnets occurs due to the induced eddy currents. The magnetic field seen by the magnets is mainly constant. However, there are some high frequency harmonics on the magnetic field crossing the magnets, created by the effect of stator slots and by high frequency current harmonics originated by PWM voltages. This alternating magnetic fields induce electromotive forces in the magnets. And as the magnets have conduction properties (they are not electrically isolated materials, but they have a resistivity) electric currents are induced. These induced currents generate losses.

The magnet losses are computed in the same way as in the case of the motor AB (see deliverable D4.1).

5.2 Cooling system

The cooling system is the same as the one implemented in the AB motor. It consists of two systems: oil through rotor cooling and oil spray cooling.

A set of cooling channels has been configured in the rotor. The oil flow is injected through the shaft hole from the front to the rear. On the rear side of the rotor, the oil flow is directed from the shaft to the rotor channels using an end plate (see the shaft hole and the rotor channels in the Figure 16). At the same time, the shaft have some holes just in front of the end windings. As the rotor rotates, a portion of the oil flowing inside the shaft is expelled through the inner face of the end windings thanks to the centrifugal forces.

In addition, the spray cooling system is applied directly to the outer surface of the end windings. This way oil is applied on both, outer and inner surfaces of the end-windings, significantly improving the heat extraction from the copper. Consequently, with this cooling system, most of the heat generated in the copper is removed through the end windings.

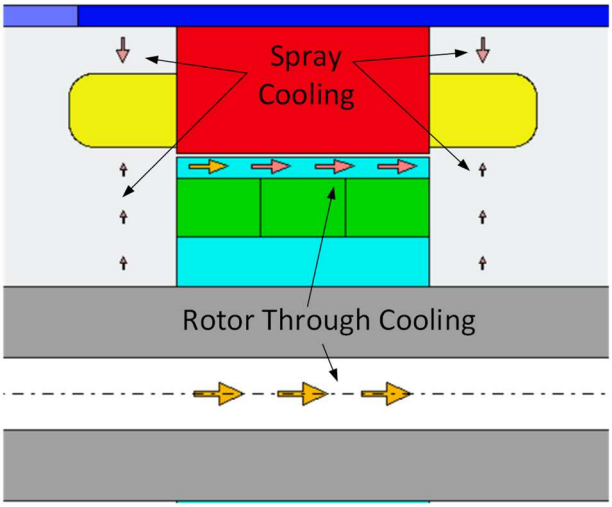

Figure 16. Description of the implemented cooling system

5.3 Continuous service curves

The continuous services curves are obtained in steady state, limiting the working temperatures at 150ºC in case of magnets, and at 180ºC in case of windings. Moreover, at each working point the current is limited in order to avoid partial demagnetization in the magnets. The demagnetization is evaluated injecting all the current in the d-axis, and the current magnitude is limited in case the demagnetization ratio is higher than 5% (working point WP Pmax).

For each working point, many iterations must be performed until the final result is obtained. In the Table 4 the results are reported. Five working points are analysed. The three points defined in the specifications (WP1, WP2, WP3), the zero-speed point (WP0) and the working point corresponding to the maximum value of the power over the continuous service curve (WP Pmax). This maximum point is located between the working points WP1 and WP2.

In the Figure 17 the continuous service curves for the power and the torque are shown. The maximum value of the power is about 186 Kw. This point is located at the speed of 8500 rpm. Thus, the motor torque at this point is around 209 Nm. This power value is used for the computation of the KPI of power density. While the torque density KPI is computed using the axel torque, which is obtained multiplying the motor torque by the gearbox ratio (1:13.5).

	WP0	WP1	WP Pmax	WP2	WP3
Current [Arms]	335,86	303,65	273,1	187,3	131,2
Phase advance [º]	50,61	50,24	59,42	73,63	79,02
Speed [rpm]	0	6250	8500	14382	19914
Shaft Torque [Nm]	269,8	240,4	209,0	95,0	40,0
Power [kW]	0,0	157,4	186,0	143,1	83,4
Magnet temperature	101,48	135,13	140,5	144,3	152,7
Winding temperature	180,12	179,97	168,4	148,9	139,4
Copper dc	9301	7592	5977	2566	1286
Copper ac	0	391,9	485,5	350,6	379
Iron Losses	0	1136	1600	2558	3503
Magnet Losses	0	48,93	63,14	110,2	121,8

Table 4. Continuous service working points computed in steady state limiting the winding temperature to 180ºC, and magnet temperature to 150ºC

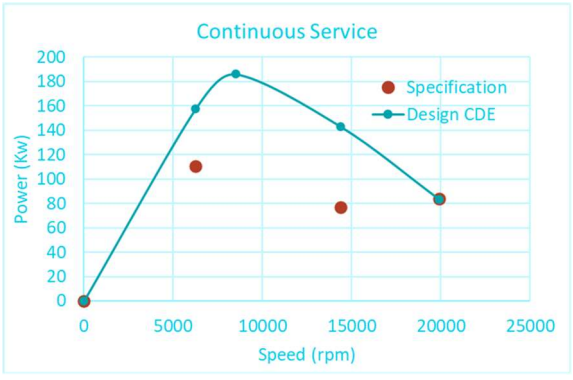

a) *Mechanical Power*

b) *Mechanical Torque*

Figure 17. Continuous service curves

It is noteworthy that at WP0, the motor is capable of delivering the peak torque value in steady state (270 Nm). At this operating point, both the rotating speed and the operating frequency are zero. Hence, the are neither iron losses nor magnet losses at zero speed, allowing the cooling

system to effectively extract all the heat and maintain working temperatures below the maximum permissible limits.

At the working point WP1, the torque capability is reduced slightly due to the thermal limitation of the winding.

At the working points WP Pmax and WP2 the torque capability is not thermally limited, but due to the demagnetization ratio. The winding and magnet temperatures are below their maximum limits, but the current magnitude is limited in order to avoid partial demagnetization of the magnets.

In the remaining working point (WP3), both iron and magnet losses increase significantly so that the copper losses must be reduced (reducing the current, and so the torque) to prevent overheating of the motor. At this working point the limiting factor is the magnet temperature, which reaches 153 ºC, slightly exceeding the maximum allowable limit.

Summarizing, the designed eMotor successfully meets all required continuous working points. The most critical working point is at the highest speed, which is achieved without any margin. On the other side, at the other working points the capability of the motor significantly exceeds the requirements.

6 FINAL PERFORMANCES AND COMPUTATION OF KPIS

6.1 Evaluation of KPIs

In this section the evaluation of the KPIs is described. The reported values are the ones corresponding to the final CDE segment motor design.

6.1.1 Computation of Weight and Volume

The weight of the electric motor is computed without and with gearbox. In the Figure 18 the considered dimensions and the elements considered as part of the motor and the ones considered as part of the gearbox are depicted. As the design of the gearbox is not part of the HEFT project scope, a base-line commercial gearbox is used to evaluate equivalent volume and weight. It is important to note that the drawing of the gearbox (Figure 18) only represents the equivalent volume of the gearbox. The final gearbox geometries for a final use have not yet been defined. Both, the bearings and the shaft are not considered part of the electric motor, but they are considered as components of the gearbox, as the final design will feature an integrated mechanical frame with axle and bearings.

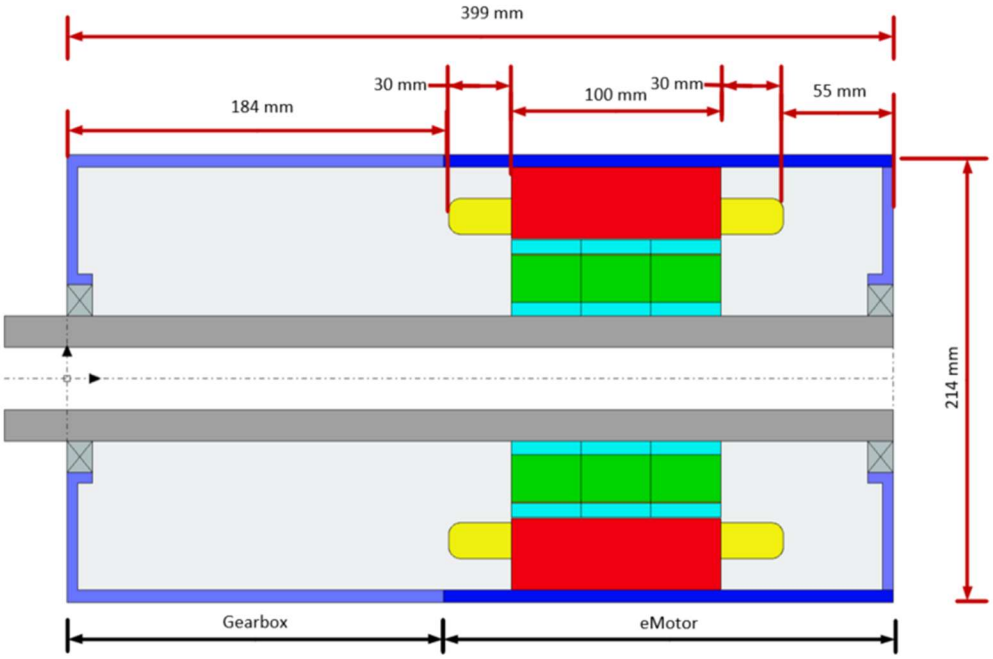

Figure 18. Main dimensions of the electric motor with a stack length of 100mm, including the gearbox

6.1.1.1 Gearbox

A commercial aluminium casing gearbox is included for the design and the front bearings and end cap are considered as part of the gearbox.

Volume	6.6 litres
Aluminium Casing Weight	4.3 kg
Total Weight	21.6 kg

Table 5. Considered weight and volume for the commercial gearbox

6.1.1.2 Stator and Rotor laminations Weight

The stator and rotor magnetic cores are made of silicon steel of grade NO 27. The density of the material is $7.6\ kg/dm^3$. Thus, the weight is computed multiplying the volume by the density. In the particular case of a stack length of $100\ mm$, the stator lamination weight is $10.07\ kg$ and the rotor lamination weight is $5.38\ kg$.

6.1.1.3 Copper Weight

The wave winding is characterized for having smaller end-windings than the conventional Hairpin. An end winding length of 30 mm is considered. In the Figure 19 the estimation of the copper weight is described. Considering rectangular conductors, the total cooper weight is 4.104 Kg. Nevertheless, the edge of the conductors is rounded, resulting in a slightly smaller weight of approximately 3.97 kg.

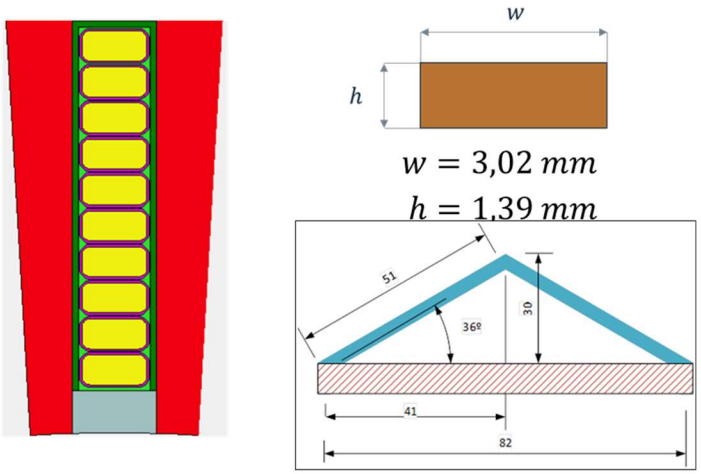

Stack length	Active Weight	End-Winding	Total Weight (Without fillet)	Total Weight (With fillet)
100 mm	2,031 kg	2,073 kg	4,104 kg	3,97 kg

Figure 19. Estimation of the copper weight

6.1.1.4 Magnet Weight

The magnet grade is N42SH. According to datasheets given by suppliers, this kind of magnets have a density of $7.5\ kg/m^3$. This way, the weight is computed multiplying the volume by the density. In the case of a stack length of $100\ mm$, the magnet weight is $1.71\ kg$.

6.1.1.5 Housing Weight

The housing is manufactured by SUMIBE's epoxy which have a density of $1.7\ kg/dm^3$. The width of the housing is set to $6\ mm$ and the length is about $215\ mm$, giving as a result a volume of $0.8429\ dm^3$, and a weight of $1.433\ kg$. These values correspond to a stack length of $100\ mm$.

6.1.1.6 Rear End Cap Weight

The rear end cap is manufactured by SUMIBE's epoxy which have a density of $1.7\ kg/dm^3$. The width of the end cap is defined to $5\ mm$. Hence, the volume of the rear end cap is $0.1436\ dm^3$, and the weight is $0.2442\ kg$. This value does not change with the stack length.

6.1.1.7 Rotor Cavity Weight

The rotor geometry includes several holes: some are designed to accommodate the magnets, while others serve cooling purposes and help reduce the overall weight of the rotor. In the assembly process of the rotor, the insertion of magnets inside the cavities requires the holes to be slightly higher and wider than the magnets. Once the magnets are put inside the cavities, fixing epoxy is injected, so that all cavities are filled completely with this adhesive product. The employed epoxy has a density of $1.97\ kg/dm^3$. The weight of the fixing epoxy is also considered. In the case of the CDE motor, the rotor cavity weight is 0.085 kg. The contribution with the fixing

epoxy to the overall motor weight is practically neglectable. However, it has been included in the study.

6.1.1.8 Total motor Weight

In the Table 6 the estimated total weight of the electric motor without considering the gearbox is reported. The contribution of each element to the total weight is expanded.

Stator Lamination	10.07 kg
Rotor Lamination	5.38 kg
Armature Copper	3.97 kg
Magnet	1.71 kg
Housing	1.43 kg
End Cap Rear	0.24 kg
Rotor Cavities	0.08 kg
MOTOR WEIGHT (without gearbox)	22.88

Table 6. Estimated weight for the motor without gearbox (stack length of 100 mm)

Motor Weight without Gearbox	22.88 kg
Bearings Weight	0.66 kg
Shaft Weight	7.03 kg
Gearbox Weight	21.60 kg
TOTAL MOTOR WEIGHT (with gearbox)	52.17 kg

Table 7. Estimated total weight for the motor with gearbox (stack length of 100 mm)

6.1.1.9 Total motor Volume

The outer diameter of the motor considering the housing is $d_o = 217mm$. The length of the motor without considering the gearbox is $l_m = 140\,mm$. Hence, the total volume of the electric motor without considering the gearbox is:

$$V_{motor} = \pi\left(\frac{d_o}{2}\right)^2 \cdot l = \pi\left(\frac{0.217}{2}\right)^2 \cdot 0.140 = 5.18\,dm^3 \quad (1)$$

The overall volume of the motor is obtained adding the volume of the gearbox to the volume of the motor. The volumes are reported in the Table 8.

Gearbox Volume	6.6 litres
Motor Volume (without gearbox)	7.73 litres
Total Motor Volume (with gearbox)	14.33 litres

Table 8. Estimated overall volume of the electric motor with gearbox (stack length of 100 mm)

6.1.2 Evaluation of Torque and Power Densities

The power and torque density are computed considering the maximum values of torque and power in the continuous service (see Table 4 and Figure 17). In case of the CDE motor, the maximum value of the power in continuous service is $P_{cs-m} = 186\,kw$. And the maximum axel torque in continuous service is $T_{cs-ma} = 2821\,Nm$ (multiplying the maximum torque of the motor, 209 Nm by the gearbox ratio 13.5).

The power density is computed without considering the gearbox. It is calculated considering the weight and the volume.

$$P_{dens}\left(\frac{kw}{kg}\right) = \frac{P_{cs-max}}{W_{motor}} = \frac{186}{22.88} = 8.13\frac{Kw}{kg}$$
$$P_{dens}\left(\frac{kw}{l}\right) = \frac{P_{cs-max}}{V_{motor}} = \frac{186}{7.73} = 24.06\ \frac{Kw}{l} \quad (2)$$

The torque density is computed considering the gearbox. It is calculated considering the weight and the volume.

$$T_{dens}\left(\frac{Nm}{kg}\right) = \frac{T_{cs-max}}{W_{total}} = \frac{2821}{52.17} = 54.08\frac{Nm}{kg}$$
$$T_{dens}\left(\frac{Nm}{l}\right) = \frac{T_{cs-ma}}{V_{total}} = \frac{2821}{14.33} = 196.85\ \frac{Nm}{l} \quad (3)$$

6.1.3 Evaluation of the REE Saving

The saving in Rare Earth Elements (REE) is computed against the REE composition of benchmark magnets employed in the reference motor ID4.

A comparison between the magnet volume and weight for both the CDE eMotor and the reference motor indicates that the CDE eMotor achieves a significant reduction in magnet weight, specifically a reduction of 37%.

It should be remarked that in the CDE eMotor a direct rotor cooling is used allowing lower rotor temperatures. The design uses N42SH grade magnets. The benchmark motor employs magnets with a higher thermal grade. By opting for a lower thermal grade, the requirement for heavy rare earth elements (HREE) are reduced, thereby contributing to the REE savings KPI.

A saving of 35% is achieved in case of Light Rare Earth Elements (LREE), being the main element the Neodymium. While a saving of 85% is achieved in case of Heavy Rare Earth Elements (HREE), being the Terbium and the Dysprosium the main elements.

To determine the overall REE savings, the weighted average value is calculated by considering the savings in both light and heavy rare earth elements. As defined in the HEFT project grant agreement, and similarly applied in the case of the AB motor, a weight of 40% is assigned to the LREE savings, and a weight of 60% is assigned to the HREE savings. The total HREE saving factor is calculated as follows

$$REE_{saving} = 0.4 \cdot ST_{LREE} + 0.6 \cdot ST_{HREE} = 0.4 \cdot 34.82 + 0.6 \cdot 84.89 = 64.86\% \quad (4)$$

6.2

6.3 Final Performances

In this section the final performances of the CDE segment motor design are reported. Figure 20 shows the resulting peak envelopes of torque and power. It can be observed that the working point at base speed meets the required specifications, while at higher speeds, the peak envelopes exceed the required values with a significant margin.

Figure 21 shows the torque and power curves for continuous service. It is noteworthy that at the highest speed working point, the motor's capability meets the required specifications. At lower speed working points, the motor's capability exceeds the requirements. The maximum power output of the motor in continuous service is 80% of the maximum power output in non-continuous service. This high value of power given in continuous service is due to the effectiveness of the cooling systems. These strong performances in continuous service enable the achievement of the power and torque density KPIs.

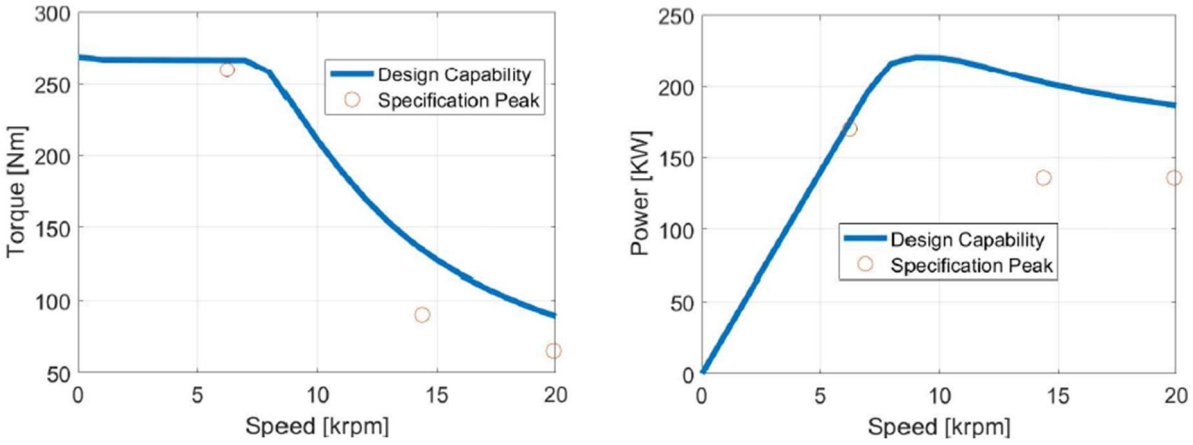

Figure 20. Peak envelope of mechanical torque and mechanical power

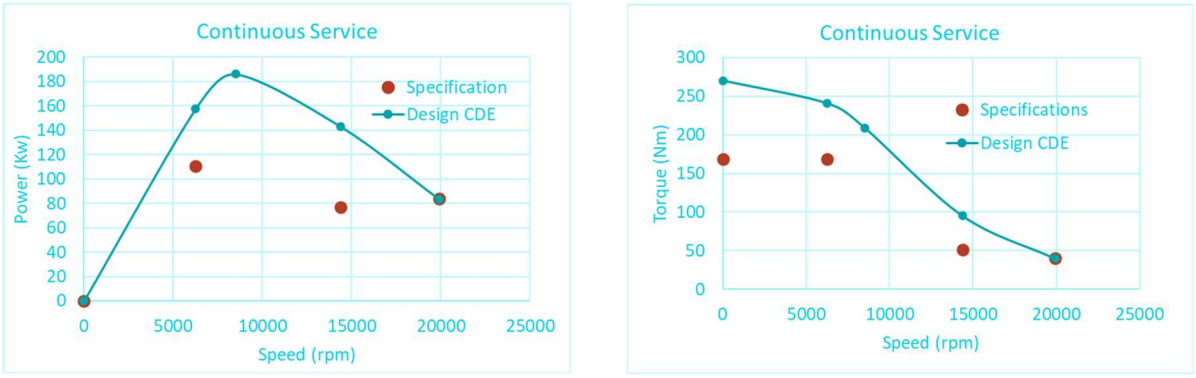

a) Mechanical Power *b) Mechanical Torque*

Figure 21. Continuous service curves

In the Figure 22 the torque waveforms computed at all characteristics working points are depicted. In all cases the peak-to-peak value of the torque ripple remains below the required maximum value ($\Delta T_{pp} < 5\%$). In the Figure 23 the torque ripple in per unit is plotted in the four working points. According to these results, it can be stated that the torque ripple requirement is fulfilled, as very low values are obtained.

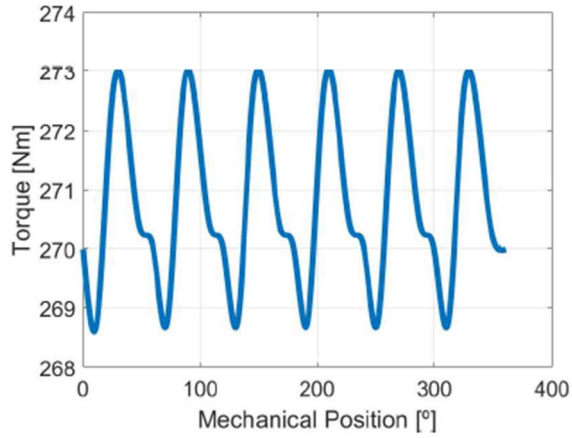

a) Working Point WP1 ($\Delta T_{pp} = 1.63\%$)

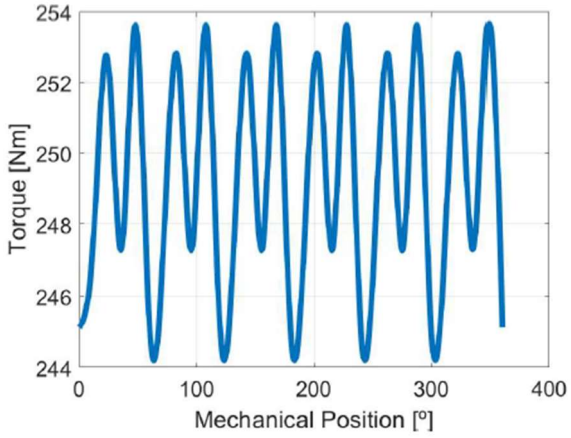

b) Working Point WP Pmax ($\Delta T_{pp} = 3.79\%$)

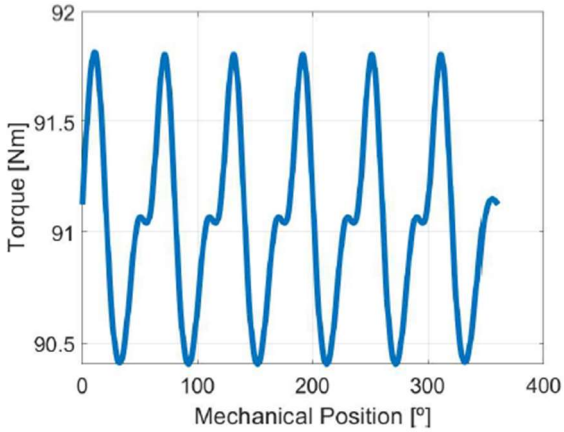

c)Working Point WP2 ($\Delta T_{pp} = 1.55\%$)

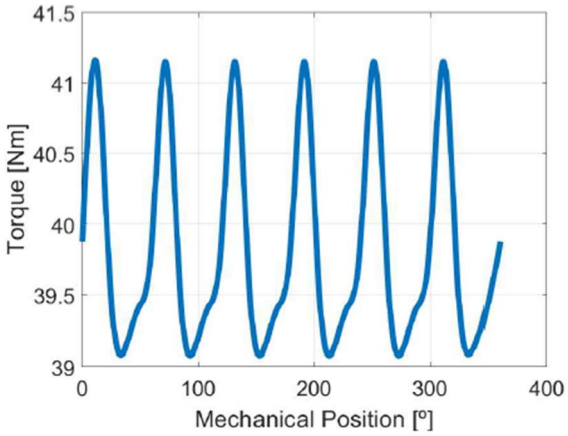

d)Working Point WP3 ($\Delta T_{pp} = 5.25\%$)

Figure 22. Torque waveforms obtained at different working points

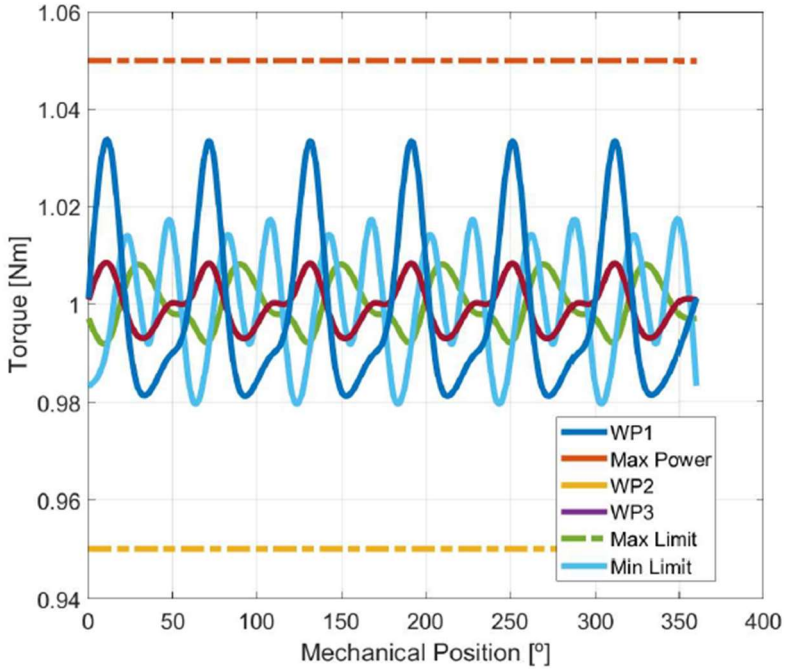

Figure 23. Torque ripple per unit computed in the different working points

Besides the main performance curves, in this chapter also the computed KPIs for the final motor design are reported. Underline that the proposed motor design fulfils all KPI's considering the defined targets.

	Call Target	GA computations	Obtained Result
Power density (kw/kg)	$> 7\ kw/kg$	$\approx 7.07\ kw/kg$	$8.13\ kw/kg$
Power density (kw/l)	$> 23 kw/L$	$\approx 43.04\ kw/L$	$24.06\ kw/L$
Torque density (Nm/kg)	$> 20\ Nm/kg$	$\approx 26.44\ Nm/kg$	$54.08\ Nm/kg$
Torque density (Nm/l)	$> 50\ Nm/L$	Non-defined	$196.85\ Nm/L$
REE Saving	$> 60\%$	$\approx 63\%$	$\sim 65\%$

Table 9. Final KPIs obtained with the eMotor design for segment CDE

7 DELIVERY DEVIATIONS FROM THE INITIAL PLANNING

There has been a delay in the delivery of D4.2 Electromagnetic and Performance. Design Report of Motor for Class C+D+E Vehicles

Contractual delivery: 2024-05-31

Deliverable Date: 2025-01-05

Technical deviations:

This delay is due to the several iterations during the design of the emotor to have an emotor capable of being manufactured by wave winding in the automatic manufacturing line available at the University of Nottingham. Priority has been given to solve earlier the problems in the design of A+B segment, in order to implement all the improvements in C+D segment.

Delay effect on overall project planning:

The delay in D4.2 has no effect on the overall project planning, because the critical prototype was the one related to A+B segment, the first to be delivered. Furthermore, most of the work was already done on the contractual date but some changes and validations have been carried out again, in order to adjust the design to the automatic manufacturing requirements.

8 CONCLUSIONS

A new motor design for CDE segment electric vehicles is reported in this document. The proposed motor design is characterized by a very high power density ($> 7\ kw/kg\ \ | > 23\ kw/l$), torque density ($> 20\ Nm/kg\ | > 50\ Nm/l$) and very low REE usage (REE saving $> 60\%$ in comparison with benchmark motors).

As main conclusion it can be stated that the proposed motor design fulfils all design requirements and KPIs defined in the call. These successful results have been possible thanks to the implementation of different novel technologies in the design of the motor: Wave windings, multibarrier IPM rotors, light epoxy materials and spray cooling.

Wave winding technology makes possible to perform very compact windings and also makes possible to insert 10 conductors inside the slot. The state of the art is about 8 conductors per slot with hairpin technology. Increasing the number of conductors inside the slots the AC losses are reduced, and more turns per phase are achieved. Increasing the number of turns per phase makes possible to reduce the required magnet flux, reducing this way the used magnet volume. Moreover, compact windings means that less copper is used leading to lighter stators.

The use of novel epoxy materials for the manufacturing of the housing makes possible to reduce considerably the weight of the housing, contributing to the consecution of the power and torque density KPIs.

The optimization of the multibarrier rotors makes possible to optimize the usage of magnets. This impact mainly to the REE saving KPI but also to the power and torque density. The less magnet weight is used, the lighter the rotor is.

The cooling channels situated near the magnets improve the heat extraction from the magnets. Moreover, the spray cooling applied over the end-windings enhances the direct heat extraction from the copper. With this cooling system rather high continuous service curves are achieved leading to high power and torque densities.